The French dual-polarization processing chain and its associated products

Abdel-Amin Boumahmoud[1], Hassan Al-Sakka[1], Jean-Louis Champeaux[1] ,

J. Figueras i Ventura[1], Béatrice Fradon[1], F. Kabeche[1], Pierre Tabary[1]

[1]Centre de Météorologie Radar, Météo France, Toulouse, France,
Corresponding author : mailto:jean-louis.champeaux@meteo.fr

1. Introduction

Quantitative precipitation estimation (QPE) is the major goal of the weather radar community since practically the beginning of the field. Traditionally, precipitation estimation has been performed using a parameterised relationship between rainfall rate R and reflectivity (typically the horizontal reflectivity Zh). However, this family of estimators suffers from large uncertainties due to:
- the variability of the drop size distribution (DSD), both in time and space,
- precipitation-induced attenuation along the path (more pronounced at C-band and even more at X-band), which leads to an underestimation of Zh, particularly at long distances and behind areas of intense precipitation
- over-estimation of reflectivity due to the presence of hail or melting snow.
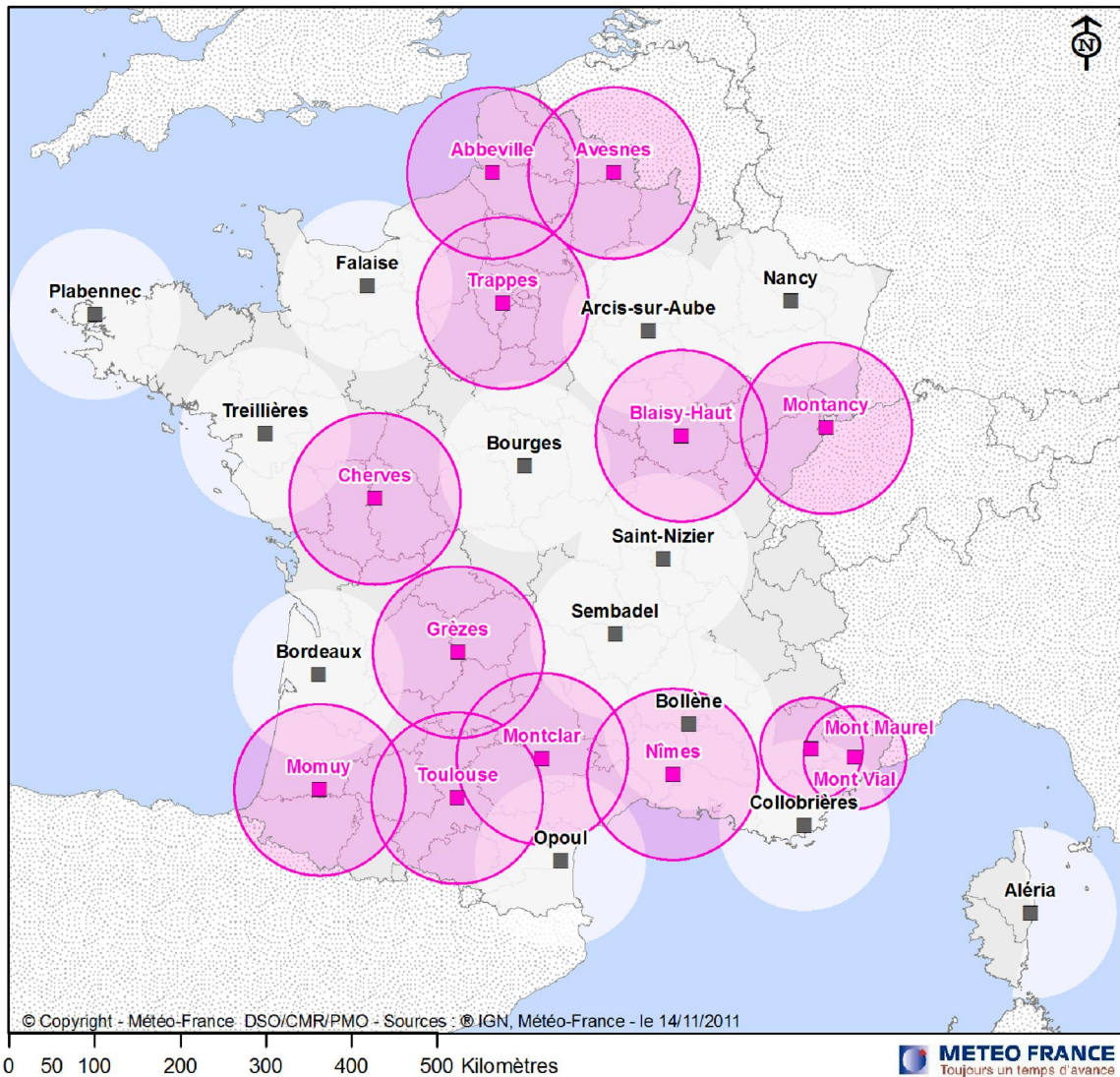In addition to those uncertainties, rainfall estimation with radars is complicated by ground-clutter effects, partial beam blocking, partial beam filling, radar calibration biases í
The extra information provided by polarimetric variables can significantly help mitigating errors (Bringi and Chandrasekar, 2001) since it allows the identification of the scatterers, the attenuation correction and the real-time retrieval of the DSD parameters. Numerous polarimetric QPE algorithms have been proposed at S, C and X-band (see Rhyzhkov et al. (2005) and Tabary et al. (2011) for a review at S- and C-band, respectively) but most of them have been tested offline in a research mode, where data selection or ex-post calibration of polarimetric variables are possible. As polarimetry is gradually being introduced introduced into operational radar networks worldwide, it appears important to revisit the advantages and drawbacks of the various algorithms in light of realistic operational measurement conditions.

Meteo-France investment on operational radar polarimetry started in 2004 with the installation of the first French polarimetric radar (C-band) in Trappes. Since then, a significant amount of work has been carried out and the positive results obtained have led to the extension of dual-polarization to other radars of the network. In 2011, 11 out of the 24 radars composing the metropolitan French weather radar network are polarimetric (10 at C-band and 1 at S-band, Fig.1). Additionally, X-band radars are being deployed in order to improve the coverage over the French Southern Alps. All radars are equipped with the same õhome-madeö radar processor (named CASTOR2), which guarantees homogeneity of the products.

   This paper describes the first version of the dual-polarization processing chain implemented for tests on the 11 polarimetric radars since July 2010 and in operational mode for 3 (Trappes, Monclar and Abbeville) of them since September 2011.

Fig. 1 The French Operational Radar Network

2. Description of the dual-polarization chain

Polarimetric variables (Z_H, Z_{DR}, Φ_{DP}, ρ_{HV}) +

Bias reference curves :

Bias curves for Z_H and Z_{DR}

Offset curves for Φ_{DP}

$Z_{DR}^{90°}$ threshold

$\rho_{HV}^{80\%}$ threshold

Calibration of Z_H and

Non meteorological echo identification

ρ_{HV}-based bright band identification

Φ_{DP} offset removal and

K_{DP} estimation

Attenuation correction

Hydrometeor classification

Daily monitoring computing

Alarm Triggered ?

Dual-polarization chain

Path Integrated Attenuation of Z_H

Echo Types

Daily means : Bias curves for Z_H and Z_{DR} Φ_{DP} offset curves

Dual-polarization products inhibition

QPE

Reflectivity pseudo-CAPPI image

í

Operational products
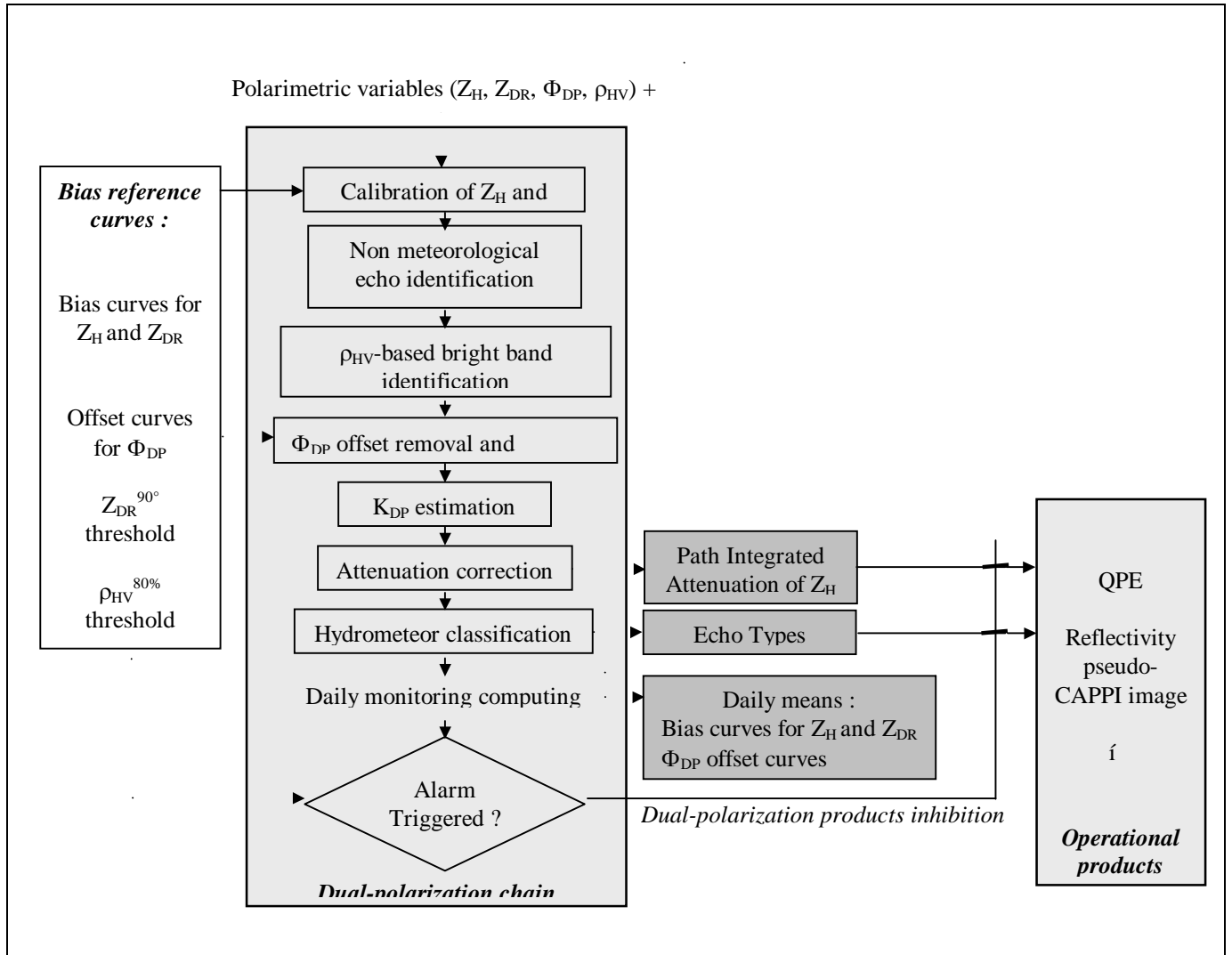
Fig. 2: Dual polarization chain

The dual-polarization chain uses raw polar ($0.5° \times 240\text{m}$) fields of Z_H, Z_{DR}, Φ_{DP}, ρ_{HV} and a Cartesian ($512 \times 512 \times 1\text{km}^2$) field of pulse-to-pulse fluctuation of reflectivity (Σ).

The polarimetric processing chain performs successively calibration of the polarimetric variables (Z_H and Z_{DR}), non meteorological echo identification, bright band identification, Φ_{DP} offset removal and filtering, K_{DP} estimation, attenuation correction and hydrometeor classification (Boumahmoud et al., 2010).

2.1. Calibration of the polarimetric variables

In its first version, only Z_{DR} is corrected. For each elevation, the correction is defined by a mean Z_{DR} azimuth curve considered as a reference and computed during a previous daily monitoring. In a subsequent version a Z_H calibration curve will be computed using the consistency approach (Gourley et al., 2009).

2.2. Non meteorological echo identification

This module (Gourley et al., 2007b) allows us to identify precipitation pixels (PR), ground clutter pixels

(GC) and clear air pixels (CA).
First we do simple tests :

- If Σ is less or equal to 2.5dB then the pixel is "GC" but if Σ is greater than 5dB then the pixel can't be "GC".
- If the beam height (assuming standard propagation) is larger than 3km (in C-band and 4.5km in S-band) then the pixel can't be classified as "CA".
- If Z_H is greater than 22dBZ (in C-band and 28dBZ in S-band) then the pixel can't be "CA".
- If ρ_{HV} is less than 0.8, Z_H less than 35dBZ and SNR greater than 20dB then the pixel can't be classified as "PR".

After all this tests, if a pixel hasn't a unique classification then we use fuzzy logic. For each type i (PR, GC, CA) a probability is computed using the probability density functions of PR, GC and CA knowing Σ, ρ_{HV} and the texture of Z_{DR} :

$$P_i = 0.4 \cdot P_i^{HV} + 0.4 \cdot P_i + 0.2 \cdot P_i^{Text\,Z_{DR}}$$

2.3. Bright band identification

The bright band identification is done comparing the real ρ_{HV} profile with theoretical ρ_{HV} profile candidates. These theoretical profiles are computed varying the freezing level height (FLH) between +- 700 m of the FLH predicted by the NWP model and varying the bright band thickness (BBT) between 200 m and 1500 m. The antenna diagram is taken into account in the simulations. The best simulated profile is that one that minimizes the Nash index with a minimum correlation of 0.9 between observed and simulated profiles (Tabary et al. 2006). The FLH and the BBT are then smoothed in time.

2.4. Φ_{DP} offset removal and filtering and K_{DP} estimation

Φ_{DP} used to be corrected by the Φ_{DP} offset computed on a previous day but observations of those parameters shown too much variability from day to day. Now the Φ_{DP} offset removal is done dynamically for each ray with the mean ϕ_{DP} computed from the 10 first consecutive available precipitation gates along the ray. On each ray, Φ_{DP} is then smoothed using a 6 km-wide median filter.
K_{DP} is determined by linear regression on the same 6 km-wide interval.

2.5. Attenuation correction and reflectivity products

Attenuation correction (both on Z_H and Z_{DR}) is done using Φ_{DP} (with constant proportionality coefficients γ_H and γ_{DP}) :

$$Z_H^{CORR} = Z_H + \gamma_H \cdot \phi_{DP}$$
$$Z_{DR}^{CORR} = Z_{DR} + \gamma_{DP} \cdot \phi_{DP}$$

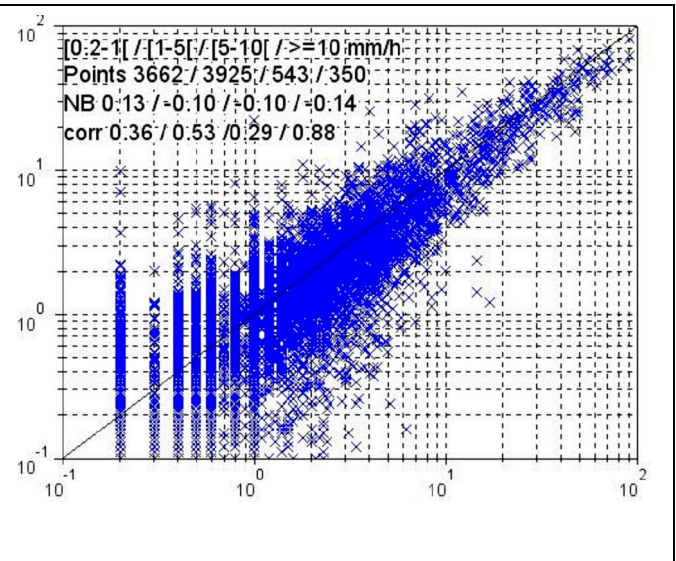C-band : $\gamma_H = 0.08$ and $\gamma_{DP} = 0.03$ (Gourley et al. 2007a)
S-band : $\gamma_H = 0.04$ and $\gamma_{DP} = 0.004$

The chain provides Cartesian outputs of the Path Integrated Attenuation (PIA) of horizontal reflectivity (Z_H) and of echo types that are subsequently used in all operational products (QPE, reflectivity pseudo-CAPPI image, …).

2.6. First results of the operational QPE with attenuation correction
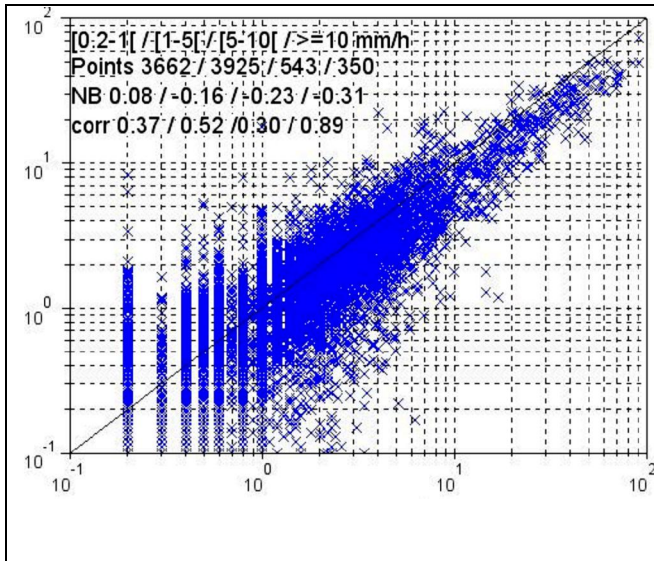
Fig. 3a: Conventional QPE without rain gauges adjustment (rain gauge (mm) in abscissa and QPE (mm) in ordinate)	Fig. 3b: Dual polarization QPE without rain gauges adjustment (rain gauge (mm) in abscissa and QPE (mm) in ordinate)

Preliminary results are presented and were obtained from 12 events. All the results are stratified according to 4 ranges on the rain gauge hourly accumulations: [0.2, 1[, [1, 5[, [5, 10[and >10 mm/h. This comparison is done on a collocated pixel basis.

The quality of the algorithms is evaluated based on the normalized bias between the rain gauge and the radar retrieved rainfall accumulation (NB) defined as:

$$NB = \frac{\langle R \rangle}{\langle G \rangle} - 1$$

R radar estimations and G rain gauges values

and the correlation (corr):

$$corr = \frac{\sum_{\forall i} \left(G_i - \langle G \rangle \right) \left(R_i - \langle R \rangle \right)}{\sqrt{\sum_{\forall i} \left(G_i - \langle G \rangle \right)^2} \sqrt{\sum_{\forall i} \left(R_i - \langle R \rangle \right)^2}}$$

Notice that for small intervals, the correlation does not provide meaningful results.

The correction of the attenuation in the first version of the QPE processing chain improved the results of normalized bias (Figures 3) and limit the under-estimation of the radar QPE particularly for the heavy rains: for instance, for rain gauge > 10mm/h, the normalized bias is ó0.31 for the conventional QPE without rain gauge adjustment and ó0.14 for dual polarization QPE without rain gauge adjustment.

3. The necessity of introducing monitoring indicators

Given the high sensitivity of dual-polarization algorithms to biases on Z_{DR}, ϕ_{DP}, ρ_{HV} and to a lesser extent Z_H, the operational introduction of dual-polarization prompted the definition and production of monitoring indicators on a daily basis. The idea was to detect as early as possible a failure in the radar system (rotary joint failure, wave guide losses, TR tube failure, í) that would cause problems on subsequent products. Several examples have been identified during the last years of dual-polarization operations at Météo France. The monitoring indicators that were designed and coded are the following (many of them are described in Gourley et al. 2006) :

- Mean Z_{DR} at 90°.
- Mean Z_{DR} in rain for Z_H between 20 and 22 dBZ at close-range and high-SNR.
- ϕ_{DP} offsets.
- Upper 80% quantile of all ρ_{HV} values in rain at close-range and high-SNR.
- Mean Z_{DR} on the 10 first 1km-wide rings.

Alerts are automatically triggered at the end of each day if one of the monitoring indicators falls outside predefined thresholds. In that case, the radar processing chain is turned back to conventional and the problem is analyzed and fixed by radar experts.

3.1. Mean Z_{DR} at 90°

The classical procedure to calibrate Z_{DR} consists in collecting data at vertical incidence while keeping the antenna rotating in azimuth. The 90° tilt is revisited every 15 minutes on all 10 French polarimetric radars. This way, even in the presence of canting of the drops or wobbling of the antenna, the intrinsic value of Z_{DR} at 90° is expected 0 dB in precipitation, so that any non-zero value is attributed to miscalibration of the radar system. The mean daily value as well as the total number of points are computed and stored. Any significant departure ($\approx\pm$ 0.5 dB) from the last available bias estimation is detected and the maintenance team is alerted. The operational use of all dual-polarization variables (Z_{DR}, ρ_{HV} and ϕ_{DP}) is inhibited until the problem has been understood.

3.2. Mean Z_{DR} in rain for Z_H between 20 and 22 dBZ at close-range and high-SNR

Recent work with operational radars (Sugier and Tabary, 2006) has clearly demonstrated the impact of the radome peel joints on the Z_{DR} measurements. These azimuth- and elevation-dependent disturbances have a typical magnitude of up to ±0.3 dB. The repeatability of the patterns (Gourley et al., 2006) suggests an empirical correction method. In that context, a new Z_{DR} calibration procedure has been proposed (Segond et al., 2007) where the intrinsic Z_{DR} of high-SNR, close-range and rainy pixels having a reflectivity between 20 and 22 dBZ is assumed to have a mean value of 0.2dB. This assumption is supported by long time series of disdrometer data in France and in the UK. Any departure from that value is considered to be a system miscalibration. The mean Z_{DR} value is this time computed both as a function of azimuth and elevation. In addition to the mean calibration bias curves, which are functions of azimuth and elevation, and are needed for correction purposes, a single mean value is computed for alerting the maintenance team, should a sudden and significant change be detected ($\approx\pm$ 0.2 dB).

3.3. Mean Z_{DR} on 1km-wide rings (up to 10 km)

At such ranges, all gates are very likely to be contaminated by ground clutter. The intrinsic value of Z_{DR} in ground clutter was empirically found to be close to zero dB ($\pm$ 3 dB). This monitoring indicator was developed to detect a TR tube failure on one of the two channels, that would cause Z_{DR} to reach unrealistically high or low values in close-ranges.
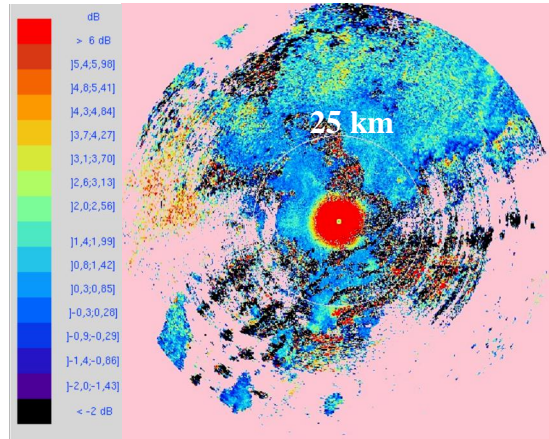
Fig. 3 Z_{DR} ó Montancy ó 7th June 2009 (TR tube failure)

3.4. ϕ_{DP} offsets

The ϕ_{DP} offset (system differential phase) is computed from the 10 first consecutive available precipitation gates along the ray. The ϕ_{DP} offset is stratified as a function of azimuth and elevation. A mean single value is computed and alerts are triggered if a sudden and significant variation with respect to the previous estimation (10°) is detected. As for the other parameters, an anomaly that is detected leads to the deactivation of dual-polarization exploitation.
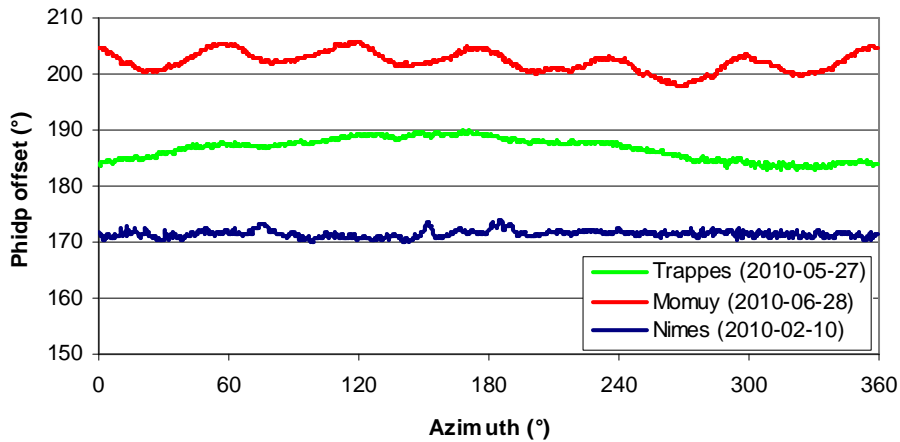

Fig. 4 ϕ_{DP} offset curve computed for Trappes (C-band), Momuy (C-band) and Nimes (S-band). Those 3 radars have different types of radome

3.5. Upper 80% quantile of all ρ_{HV} values in rain at close-range and high-SNR

A 0.99 value is expected in that case. The reason for taking the upper 80% quantile of the qualifying pixels is the very asymmetrical distribution of ρ_{HV}, which makes a few percent of outliers have a devastating influence on the simple mean and even median averages. Any significant drop of the mean ρ_{HV} in rain (below 0.95) is considered as a failure.

4. R&D products

4.1 Hydrometeor classification

This classification is only done for pixels classified as õprecipitationö during the õNon meteorological echo identificationö module (cf. §2.2). At C-Band, 10 different types are tested : light rain (LR), moderate rain (MR), heavy rain (HR), large drops (LD), wet snow (WS), dry snow (DS), ice (IC), graupel (GR), hail (HA), rain and hail mixture (RH). For every echo type, a probability, function of Z_H,

$$P_i = F_i^{Z_H}(Z_H) \cdot F_i^{T}(T) \cdot \left(1 \cdot F_i^{Z_{DR}}(Z_H, Z_{DR}) + 0.5 \cdot F_i^{K_{DP}}(Z_H, K_{DP}) + 2 \cdot F_i^{HV}(_{HV}) + 2 \cdot F_i^{BB}(h, FLH, BBT) \right)$$

Z_{DR}, ρ_{HV} ,K_{DP}, the temperature (T), the beam height (h), the freezing level height (FLH) and the bright band thickness (BBT), is computed :

where P_i is the probability that the pixel considered is of type i and F_i is a membership function used for type i.

At S-band, the hydrometeor classification algorithm (Park et al. 2009) uses the following aggregation

$$P_i = \frac{ {}_i^{Z_H} \cdot F_i^{Z_H}(Z_H) + {}_i^{Z_{DR}} \cdot F_i^{Z_{DR}}(Z_H, Z_{DR}) + {}_i^{K_{DP}} \cdot F_i^{K_{DP}}(Z_H, K_{DP}) + {}_i^{HV} \cdot F_i^{HV}(_{HV})}{ {}_i^{Z_H} + {}_i^{Z_{DR}} + {}_i^{K_{DP}} + {}_i^{HV}}$$

to determine the likelihood of a type :

where P_i is the probability that the pixel considered is of type i, F_i is a membership function used for type i and ω_i is a weight between 0 and 1 assigned to type i.

The HM classification scheme is still under development (Al-Sakka et al, 2011). The objective is to arrive at a generic approach applicable to all wavelengths with the smallest possible number of tuning parameters (weights, í).
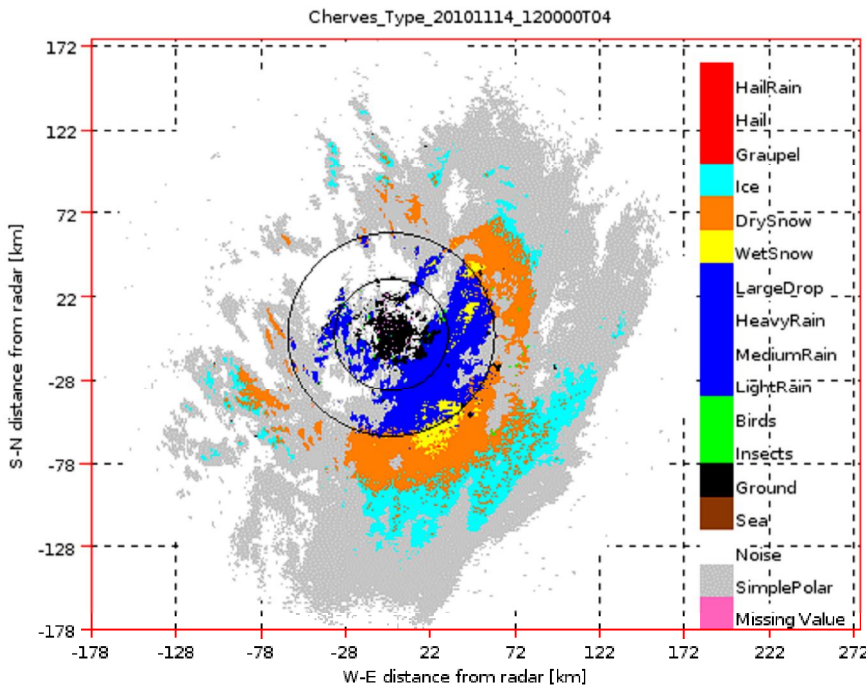

Fig. 3: Example of the classification using the old approach of classification, Cherves Radar (C-band), Météo France, 2010/11/14, 12:00, 1° of elevation.

4.2. R&D QPE processing chain

A polarimetric QPE processing chain, designed for evaluation purposes, that obtains hourly precipitation accumulation estimation from single tilts has been implemented (Figueras et al., 2011). Its flow diagram is shown in Fig. 4.
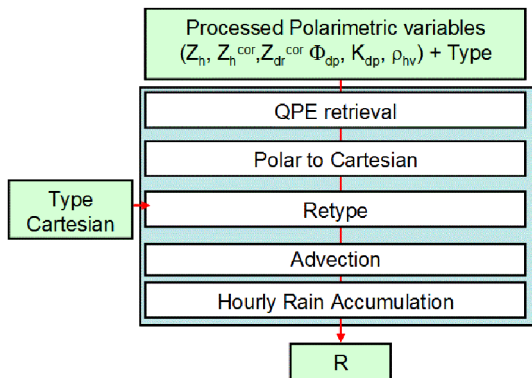

Fig.4: Flow diagram of the QPE processing

The inputs of the algorithm evaluation are the outputs of the polarimetric pre-processing chain. The first step is to estimate the instantaneous rainfall rate in areas classified as precipitation using one of the implemented algorithms. The outputs of the algorithm are then transformed from polar to Cartesian coordinates. At this point the data is re-evaluated according to the echo type. Pixels classified as noise, single polarization (low SNR), sea clutter and clear air are re-assigned from missing value to 0 mm/h rainfall rate. To compensate for the advection between measurements a temporal interpolation is performed using an advection field calculated a priori from the evolution of the previous reflectivity measurements. The interpolated rainfall rate field is added and thus the 5 minute precipitation accumulation is obtained. It follows the addition of the 12 õ5 minute precipitationö accumulation fields to obtained the hourly rainfall accumulation. The hourly rainfall accumulation can then be compared with the hourly rainfall accumulation obtained by the high density network of rain gauges operated by Météo France.

4.3. Polarimetric QPE algorithms

Polarimetric QPE algorithms are either based on horizontal reflectivity Zh, on differential reflectivity Zdr, on specific differential phase Kdp or on a combination of two or three of those parameters.

We have tested 10 algorithms that have been included in the evaluation exercise are:
- The Marshall-Palmer $Zh=200R^{1.6}$ relationship without attenuation correction;
- The Marshall-Palmer $Zh=200R^{1.6}$ relationship with attenuation correction;
- The Fulton et al. (1998) $Zh=300R^{1.4}$ relationship without attenuation correction;
- The Fulton et al. (1998) $Zh=300R^{1.4}$ relationship with attenuation correction;
- The Illingworth and Thompson (2005) Z-Zdr algorithm without attenuation correction;
- The Illingworth and Thompson (2005) Z- Zdr algorithm with attenuation correction;
- The Beard and Chuang (1987) R-K_{dp};
- The Brandes et al. (2002) R-K_{dp};
- A synthetic Z_h-K_{dp} algorithm with a 0.5 ° km^{-1} K_{dp} threshold;
- A synthetic Z_h-K_{dp} algorithm with a 1 ° km^{-1} 1 K_{dp} threshold;

The 10 Pol-QPE algorithms are evaluated offline on a number of selected [radar;day].
The 10 algorithms that have been tested are: simple Z-R relationships (Marshall-Palmer and WSR88D) with and without attenuation correction, an algorithm based on the relation between Zh and Zdr (with

and without attenuation correction), algorithms based on Kdp solely, an algorithm based on a combination of Kdp at high Kdp (above $1°$ km^{-1}) and attenuation-corrected Zh at low Kdp (below $1°$ km^{-1}). The evaluation confirms the benefits brought by polarimetry to quantitative rainfall rate estimation with radars. The attenuation correction significantly reduces the negative bias obtained with standard Zh-R relationships, specially for the highest hourly rainfall accumulations.

5. Conclusion

This paper has presented the current status of development of a polarimetric radar network data processing chain to provide accurate QPE.

The polarimetric processing chain performs successively calibration of the polarimetric variables (Z_H and Z_{DR}), non meteorological echoes identification, bright band identification, path-integrated attenuation and differential attenuation correction, Φ_{DP} offset removal and filtering (using a running 6 km median filter), K_{DP} estimation and hydrometeor classification. In its first version, the Φ_{DP} offset removal is done dynamically for each ray and attenuation correction (both on Z_H and Z_{DR}) is done using Φ_{DP} (with constant proportionality coefficients γ_H and γ_{DP}). Decision was made not to use Z_{DR} in this first version because the experience of more than one year of monitoring indicator production on the 11 radars has revealed that the current calibration / stability of Z_{DR} was close to but still below the requirement (+/- 0.2 dB) for robust and accurate quantitative exploitation. The first version of the polarimetric chain provides Cartesian outputs of the Path Integrated Attenuation (PIA) of horizontal reflectivity (Z_H) and of echo types that are subsequently used in all operational products (QPE, reflectivity pseudo-CAPPI image, í). The R&D work is continuing testing several new polarimetric QPE algorithms and the first results are positive. Furthermore, the work is going on for hydrometeor classification where determination of hail and snow are important topics.

References

Alsakka H., F. Kabeche, J. Figueras i Ventura, B. Fradon, A. A. Boumahmoud, and P. Tabary., 2011: A simple-but-realistic fuzzy logic hydrometeor classification scheme for the French X, C and S-band polarimetric radar. In Proceedings of 35nd Conference on Radar Meteorology, Pittsburgh, PA, 26-30 Sept. 2011 *American Meteorological Society: Boston.* MA.

Beard KV, Chuang C., 1987: A New Model for the Equilibrium Shape of Raindrops. *J. Atmos. Sci.* 44: 1509-1524.

Boumahmoud A.-A., Fradon B., Roquain P., Perier, L., Tabary P., 2010: French operational dual-polarization chain. European Conference on Radar in Meteorology and Hydrology. *ERAD2010.*

Brandes EA, Ryzhkov AV, Zrnic DS., 20012002?: An Evaluation of Radar Rainfall Estimates from Specific Differential Phase. *J. Atmos. Oceanic Technol.*, 18: 363-375.

Bringi V.N., Chandrasekar V., 2001: Polarimetric Doppler Weather Radar: Principles and Applications. *Cambridge University Press.*

Figueras i Ventura J, Boumahmoud A-A, Fradon B, Tabary P., 2011: Long-term monitoring of French polarimetric radar data quality and evaluation of several polarimetric quantitative precipitation estimators in ideal conditions for operational implementation at C-band. Submitted to Quarterly Journal of the Royal Meteorological Society.

Gourley, JJ, P. Tabary, J. Parent-du-Chatelet, 2006: Data quality of the Météo France C-band polarimetric radar, *J. Atmos. Oceanic Technol* , **vol. 23**, No. 10, 1340ó1356.

Gourley, JJ, P. Tabary, J. Parent-du-Chatelet, 2007a: Empirical estimation of attenuation from differential propagation phase measurements at C-band, *J. Appl. Meteor.*, **vol. 46**, No. 3, 306 ó 317.

Gourley, JJ, P. Tabary, J. Parent-du-Chatelet, 2007b: A fuzzy logic algorithm for the separation of precipitating from non-precipitating echoes using polarimetric radar, *J. Atmos. Oceanic Technol.,* **vol. 24**, Issue 8, 1439ó1451.

Gourley, JJ., A.J. Illingworth and P. Tabary, 2009 : Absolute calibration of radar reflectivity using redundancy of the polarization observations and implied constraints on drop shapes, *J. Atmos. Oceanic Technol.*, **vol. 26**, Issue 4 (April 2009) pp. 689ó703.

Illingworth A.J., Thompson R.J., 2005: The Estimation of Moderate Rain Rates with Operational Polarisation Radar. Proceedings of the 32th Conference on Radar Meteorology.

Park et al., 2009 : The hydrometeor Classification Algorithm for the Polarimetric WSR-88D : Description and Application to an MCS. *Weather and Forecasting*, **vol. 24**, pp. 730-748.

Ryzhkov A, Giangrande SE, Schuur TJ. 2005. Rainfall Estimation with a Polarimetric Prototype of WSR-88D. J. Appl. Meteor. 44: 502-515.

Segond M.-L., P. Tabary and J. Parent du Châtelet, 2007 : Quantitative precipitation estimations from operational polarimetric radars for hydrological applications, *Preprints, 33rd Int. Conf. on Radar Meteorology*, AMS, Cairns, Australia, August 2007.

Sugier, J., and P. Tabary, 2006: Evaluation of dual-polarization technology at C-band for operational weather radar network. *Report of the EUMETNET Opera 2*, Work packages 1.4 and 1.5, Deliverable b [available at http://www.knmi.nl/opera], 44 pp.

Tabary, P., A. Le Henaff, G. Vulpiani, J. Parent-du-Châtelet and J.J. Gourley, 2006: Melting layer characterization and identification with a C-band dual-polarization radar: a long-term analysis. *Proceedings of the 4th European Radar Conf.*, Barcelona, 18-22 September.

Tabary P, Boumahmoud A-A, Andrieu H, Thompson RJ, Illingworth AJ, Le Bouar E, Testud J. 2011. Evaluation of two õintegratedö polarimetric Quantitative Precipitation Estimation (QPE) algorithms at C-band. J. of Hydrology. In press.

Testud, J., Le Bouar E., Obligis E., and Ali-Mehenni M., 2000: The rain profiling algorithm applied to polarimetric weather radar, *J. Atmos. Oceanic Technol.*, Vol. 17, 332-356.